ELSEVIER

Polymer 40 (1999) 2889–2902

polymer

Spectroscopic analysis of transition-metal coordination complexes based on poly(4-vinylpyridine) and dichlorotricarbonylruthenium(II)

Mary Pat McCurdie, Laurence A. Belfiore*

Polymer Physics and Engineering Laboratory, Department of Chemical and Bioresource Engineering, Colorado State University, Fort Collins, CO 80523, USA

Received 9 January 1998; revised 9 June 1998; accepted 13 June 1998

Abstract

The formation of coordination complexes between the nitrogen lone pair on poly(4-vinylpyridine) and the metal center in dichlorotricarbonylruthenium(II) is described in this research contribution. $\{RuCl_2(CO)_3\}_2$ was chosen because octahedral d^6 heavy-metal centers with π-acid carbonyl ligands exhibit very large ligand field stabilization energies which enhance the glass transition temperatures of polymeric coordination complexes. Relative to undiluted poly(4-vinylpyridine), which exhibits a glass transition at 145°C, T_g increases by 27°C at 3 mol% Ru^{2+}. When the concentration of Ru^{2+} is greater than 5 mol%, detection of a diffuse T_g above 200°C is difficult via calorimetry because the discontinuity in specific heat decreases considerably. Ambient-temperature infrared spectroscopic data for the pyridine sidegroup in the polymer suggest that the pyridine nitrogen coordinates to ruthenium. Symmetry considerations and high-temperature infrared data for the carbonyl stretching vibrations are consistent with structural models which contain two CO ligands and two pyridine sidegroups or three CO ligands and 1 pyridine sidegroup in the coordination sphere of ruthenium. Hence, it is possible that the transition-metal salt bridges two different chains via the pyridine nitrogen lone pair, forming coordination crosslinks. Hindered mobility of this nature provides a reasonable explanation for the enhancement in T_g by 9°C/mol% Ru^{2+}, up to 3 mol% Ru^{2+}. Ambient temperature infrared signals in the carbonyl region suggest that as many as five different ligand arrangements of the following pseudo-octahedral complex, $RuCl_2(CO)_2(Py)_2$, exist simultaneously at low Ru^{2+} concentrations and could be responsible for coordination crosslinks. Upon heating, the highly symmetric isomers with *trans*-CO ligands transform irreversibly to pseudo-octahedral structures with lower symmetry (i.e., *cis*-CO ligands). Octahedral ruthenium d^6 salts are attractive physical property modifiers when polymeric ligands coordinate to the metal center.

Keywords: Poly(4-vinylpyridine); Divalent ruthenium salts; T_g enhancement

1. Introduction

Transition metal coordination is an attractive mechanism to compatibilize polymer blends that would otherwise exhibit phase separation [1–3]. Previous research has demonstrated that thermophysical properties are modified synergistically when polymeric ligands occupy sites in the coordination sphere of the transition metal [4–7]. This class of strongly interacting ''blends'' and complexes offers the materials scientist an alternative to hydrogen-bonded systems from the viewpoint of (i) physical property modifiers and (ii) miscibility enhancers. Octahedral divalent ruthenium is an attractive candidate to form coordination complexes with the pyridine nitrogen lone pair in the sidegroup of poly(4-vinylpyridine) or copolymers containing 4-vinylpyridine repeat units [4] because this transition metal has a low-spin d^6 electronic configuration and, hence, a large ligand field stabilization energy. The transition metal salt employed in this research, dichlorotricarbonylruthenium(II), maintains a pseudo-octahedral (i.e., six coordinate) geometry (i) in the undiluted state with two metal centers connected by a dichloride bridge [8], and (ii) after the dimer is cleaved by a strong base [9]. When the geometry is octahedral and the electronic configuration is d^6 in the strong-field limit, complexes exhibit energetic stabilization of these metal d-electrons with respect to the free divalent metal ion. The ligand field stabilization energy is 240% of the energy difference between the t_{2g} and e_g molecular orbitals for d^6 systems with local octahedral symmetry [10]. Furthermore, the $e_g - t_{2g}$ energy difference, or the ligand field splitting, increases when (i) a heavy metal like ruthenium is present from the second-row of the d-block, (ii) stronger σ-donors like pyridine occupy the vacant site in

* Corresponding author. Tel.: +1-970-491-5395; Fax: +1-970-491-7369; e-mail: belfiore@engr.colostate.edu

0032-3861/99/$ - see front matter
PII: S0032-3861(98)00486-8

the coordination sphere of ruthenium after the dichloride bridge is cleaved, and (iii) π-back-donation to Lewis acid-type carbon monoxide ligands lowers the energy of the t_{2g} metal-based molecular orbitals, thereby increasing the ligand field splitting [10,11]. Hence, one predicts that d^6 octahedral complexes of ruthenium with poly(4-vinylpyridine) might exhibit larger enhancements in the glass transition temperature relative to the undiluted polymer, in comparison with octahedral d^8 nickel complexes [12] and tetrahedral d^7 cobalt complexes [4] which have been studied previously in our laboratory.

Two ligand arrangements [8,9] of the dimer of dichlorotricarbonylruthenium(II) are illustrated in Fig. 1. The research strategy to produce polymeric coordination complexes, which exhibit synergistic thermal properties, is based on fundamental studies of small-molecule organometallics [13]. A strong borderline base such as pyridine will cleave the dichloride bridge and occupy the vacant octahedral site in the coordination sphere of Ru^{2+} [9], which is a borderline acid [14]. If a second pyridine sidegroup in the polymer also coordinates to the metal, then it displaces a carbonyl ligand [9], which is classified as a soft base [14]. One attractive reason for selecting the ruthenium dimer for this study is that infrared spectroscopy of the carbonyl ligands provides information about metal–ligand σ-bonding, molecular symmetry and the number of CO ligands in the coordination sphere [10]. The CO bond is weakened when π-back-donation from the metal center causes electron density to flow from the t_{2g} orbitals of ruthenium to the empty π^* antibonding orbital of carbon monoxide [10]. This antibonding orbital of CO has a larger amplitude on the carbon atom [10] which is bonded to ruthenium. Hence, there is sufficient t_{2g}-π^* overlap via molecular symmetry and proximity to accommodate π-backbonding.

The characteristic infrared stretching frequencies of terminal CO ligands lie between 1900 and 2150 wavenumbers [10]. There is a signal at 1940 cm^{-1}, due to poly(4-vinylpyridine), which does not overlap the CO absorptions of the ruthenium salt too much. Infrared shifts in the CO absorptions have been used to measure the enthalpy of acid–base reactions for polymers in various solvents [15]. When strong σ-donors like pyridine coordinate to ruthenium, the CO absorptions shift to lower energy due to π-back-donation [4,10], as described above. Benedetti et al. [9] have studied dimers of dihalobis(halotricarbonylruthenium) via infrared spectroscopy in various solvents. Carbon monoxide, triphenylphosphine, pyridine and various nitriles cleave the dihalogen bridge and occupy the vacant octahedral site in the coordination sphere of Ru^{2+} [9]. In the presence of excess pyridine, six-coordinate complexes, with Ru^{2+} at the center of the C_{2v} point group, are generated which contain two pyridine ligands in a *cis*-configuration, two carbonyls in a *cis*-configuration, and two halides in a *trans*-configuration, as illustrated in Fig. 2.

Forster and Vos [16] synthesized osmium- and ruthenium-containing metallo-polymers based on poly(4-vinylpyridine) [P4VP] and poly(*N*-vinylimidazole) [PNVI] with enhanced glass transition temperatures. The synthetic approach exploited chemical reactions between metal–bis(2,2′-bipyridyl) centers and preformed vinyl polymers *without* the formation of crosslinks to generate soluble complexes. Calorimetric data reveal that glass transition temperatures are enhanced significantly, relative to the undiluted vinyl polymers. Maximum synergy for osmium/P4VP is 109°C and the largest enhancement for osmium/PNVI is 96°C [16]. No corresponding data were reported for the ruthenium-based polymers. These ruthenium complexes were synthesized for potential photoconductor applications. There are several examples of new materials which exhibit attractive photoconductor properties. Bourdeland et al. [17] and Denti et al. [18] describe a class of materials based on ruthenium and pyridine with photoconductive characteristics. In this contribution, polymeric complexes with synergistic thermal properties can be developed if the transition-metal salt functions as a bridge between pyridine sidegroups on two different chains. This ‘‘coordination crosslink’’ configuration is illustrated in Fig. 2 where Ru^{2+} coordinates to two pyridine pendant groups with local C_{2v} symmetry. The results in this study do not provide unequivocal proof that this particular complex exists. However, infrared spectra presented herein, together with the conclusions of Benedetti et al. [9] suggest that the two CO ligands are *cis*- to each other, for the complexes that are most stable, as illustrated in Fig. 2.

Spectroscopic methods are sensitive to phase behavior when a signal from the ‘‘key component’’ is influenced strongly by neighboring components in a blend or complex. In some cases, a spectroscopic probe can detect phase coexistence when one of the phases is transparent to more conventional probes, such as thermal analysis. For example, when the melting point depression phase boundary converges with the glass transition phase boundary as the crystallizable component is diluted by the non-crystalline component, thermal analysis might only reveal the dominant glass transition which overlaps a weak melting endotherm at the same temperature [19,20]. If the key component is present in the disordered crystalline and dominant amorphous phases, and if the interaction between dissimilar species in the amorphous phase is strong enough, then infrared or solid-state NMR spectroscopies will detect phase coexistence because the signal for the key component in each environment is distinct. Hence, the overlap between T_g and T_m, as described above, is circumvented because the crystalline and amorphous regions are characterized by key component signals at (i) different NMR chemical shifts or (ii) different vibrational frequencies. When eutectic phase behavior occurs, thermal analysis reveals one melting endotherm for a two-phase mixture at the eutectic composition. This is misleading because both phases which comprise the eutectic mixture melt incongruently at the same temperature with no excess of either phase. In off-eutectic mixtures, the excess phase melts at a higher temperature to

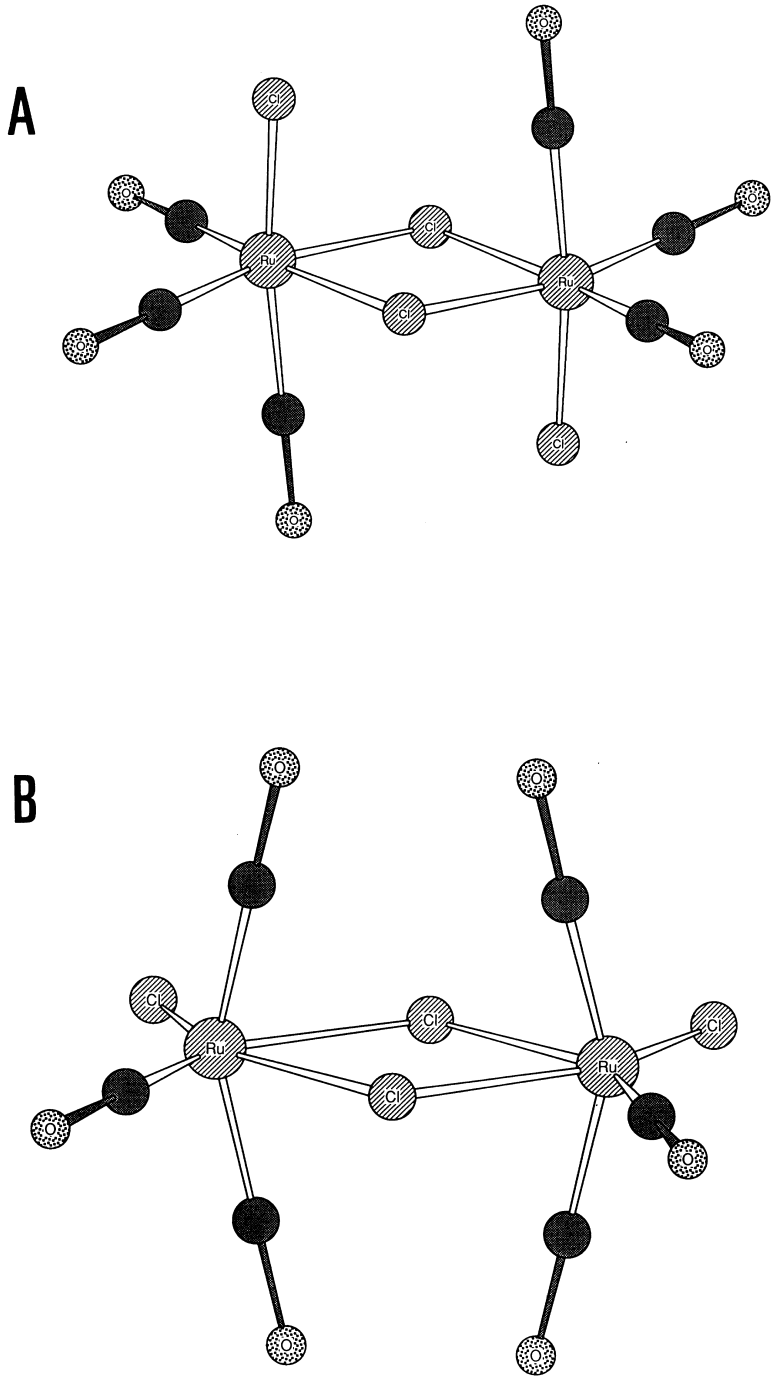

Fig. 1. Two isomers of dichlorotricarbonylruthenium(II) dimer with (A) C_{2h} symmetry and (B) C_{2v} symmetry. The isomer with C_{2h} symmetry exhibits three infrared-active C≡O stretches which belong to the following irreducible representations in C_{2h}; $A_u + 2B_u$. The isomer with C_{2v} symmetry exhibits five infrared-active C≡O stretches which belong to the following irreducible representations in C_{2v}; $2A_1 + 2B_1 + B_2$. In both cases, crystal structure studies [8,9] indicate that a dichloride bridge connects both ML_4 fragments in a pseudo-octahedral configuration.

produce a thermogram that reveals two endotherms. In both eutectic and off-eutectic mixtures of poly(ethylene oxide) with either resorcinol [21] or 2-methylresorcinol [22], ^{13}C solid-state NMR spectroscopy detects phase-sensitive signals of the small-molecule aromatic in each phase. Hence, the number of NMR absorptions for chemically identical carbon sites in the resorcinol derivatives correlates with the number of coexisting phases. However, the number of phases does not correlate with the number of melting endotherms in the differential scanning calorimetry (DSC) trace at the eutectic composition. There are other examples of crystalline–amorphous polymer–polymer blends where calorimetry and ^{13}C solid state NMR have been employed, in harmony, to probe polyester crystallinity and hydrogen

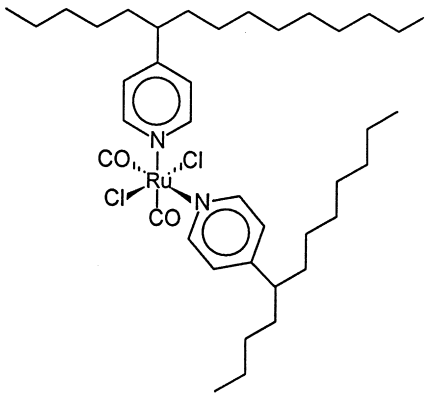

Fig. 2. A ruthenium bridge between pyridine ligands on two different polymer chains illustrates the concept of coordination crosslinking. Ligand geometry in the coordination sphere of ruthenium is adopted from the structure of $RuCl_2(CO)_2(C_5H_5N)_2$ proposed by Benedetti et al. [9]. Pyridine sidegroups are *cis*-, CO ligands are *cis*-, and the chlorides are *trans*. Local C_{2v} symmetry exists about the metal center. See Fig. 9(b).

bonding [23]. In this contribution, an infrared signal for the ''free'' ruthenium dimer at 1637 cm^{-1} is detected in coordination complexes with poly(4-vinylpyridine), when the concentration of Ru^{2+} is 10 mol% and higher (see Fig. 5). Thermal analysis is only useful to detect T_g when the concentration of Ru^{2+} is 3 mol% or less, because the glass transition becomes more diffuse and the discontinuity in specific heat at T_g is difficult to detect at higher concentrations of Ru^{2+}. Hence, $\{RuCl_2(CO)_3\}_2$ increases the T_g of poly(4-vinylpyridine) at low salt concentrations, but calorimetry cannot detect a glass transition temperature that is insensitive to Ru^{2+} concentrations above 10 mol%, if phase separation occurs.

2. Experimental considerations

2.1. Materials

The dimer of dichlorotricarbonylruthenium(II) was purchased from Aldrich Chemical Company in Milwaukee, WI. Poly(4-vinylpyridine), MW = 200 K, was obtained from Scientific Polymer Products in Ontario, NY. All materials were blended as received from the commercial distributors without further purification. The solvents used were reagent grade.

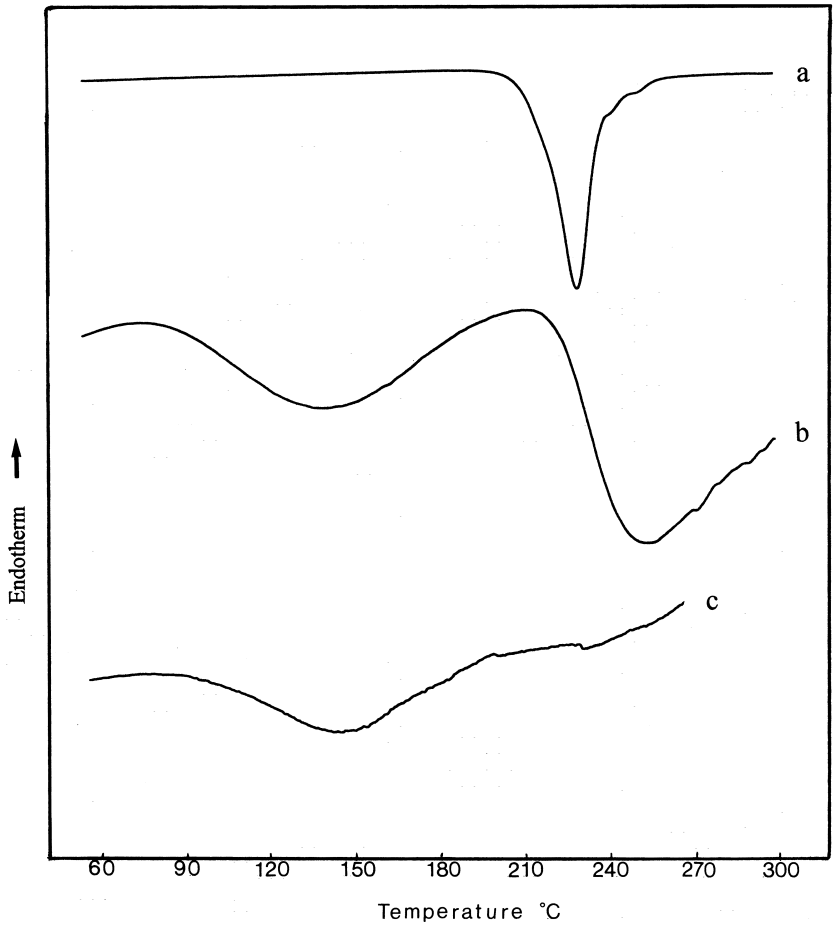

Fig. 3. Differential scanning calorimetry thermograms for (a) the undiluted ruthenium dimer, (b) a P4VP/Ru^{2+} complex containing 3 mol% Ru^{2+} and (c) undiluted poly(4-vinylpyridine), illustrating exothermic behavior during the first-heating scan in the calorimeter at a rate of 20°C min^{-1}.

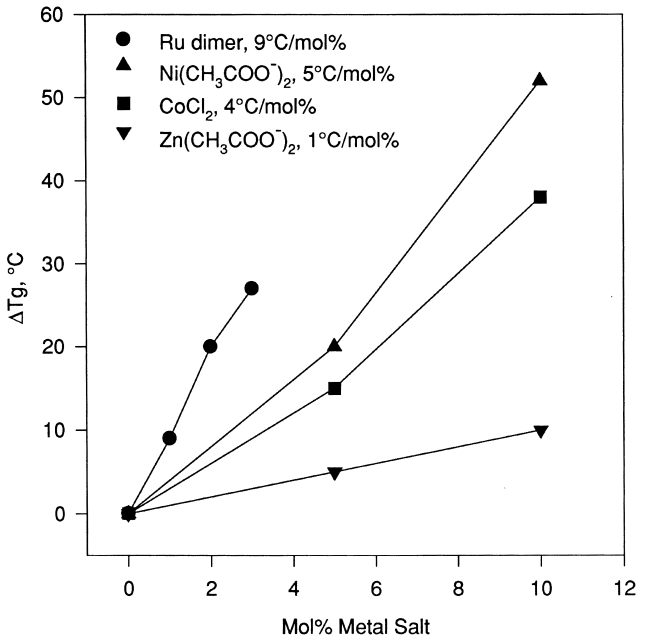

Fig. 4. Synergistic enhancement of the glass transition temperature in poly(4-vinylpyridine) coordination complexes with (a) dichlorotricarbonylruthenium(II) (circles), (b) nickel acetate tetrahydrate (upright triangles), (iii) cobalt chloride hexahydrate (squares) and (iv) zinc acetate dihydrate (inverted triangles). The vertical axis reveals the increase in T_g relative to that of undiluted P4VP (i.e., ≈145°C). The ruthenium salt produces the largest enhancement in T_g per mol% of the inorganic component.

2.2. Sample preparation methods

Poly(4-vinylpyridine) and the ruthenium salt were blended via dilute solution procedures in methylene chloride at ambient temperature. Methylene chloride was one of the solvents employed by Benedetti et al. [9]. In each case, the total mass (i.e., grams) of solids per 100 ml of solvent was approximately 2%. Solvent evaporation was accomplished via air-drying at ambient temperature in a fume hood for 24–72 h. Solid residues were subsequently dried under vacuum for 24–48 h at 60°C. Table 1 summarizes the visual observations of (i) solutions and (ii) solid complexes, after drying. Cloudy solutions were not filtered prior to recovering the solid complexes. As indicated, some of the solutions were prepared under a nitrogen purge. The reported salt concentrations in mol% refer to the moles of single Ru^{2+} metal centers (not the dimer), with respect to the repeat unit of poly(4-vinylpyridine).

2.3. Differential scanning calorimetry (DSC)

Glass transition temperatures were measured on a Perkin-Elmer DSC-7 at a rate of 20°C min^{-1} during the second or third heating trace in the calorimeter under a nitrogen purge. T_g was calculated at the midpoint of the heat capacity change between the liquid and glassy states, without complicating effects due to enthalpy relaxation. Differential power output was monitored via a Perkin Elmer TAC 7/DX thermal analysis controller in conjunction with the DSC-7 multitasking software on a 386/33 home-built personal computer. In the definitive references for ruthenium–pyridine complexes [8,9], a nitrogen atmosphere was employed during preparation in solution. To determine if the nitrogen purge was necessary during sample preparation, twelve samples at 1 mol% Ru^{2+} were prepared and tested in random order. Six of these were prepared under nitrogen and the remaining six were prepared in air. The average T_g of the N_2-purged samples was 152.5 ± 4.0°C, whereas the average T_g of the samples prepared in air was 152.7 ± 4.3°C. Hence, one concludes that a nitrogen purge is unnecessary during sample preparation because the average glass transition temperatures and their variances are essentially the same. None of the samples containing less than 5 mol% Ru^{2+} was compression molded at high temperature prior to DSC testing.

2.4. Infrared spectroscopy

FT-IR spectra of undiluted poly(4-vinylpyridine) and P4VP/Ru^{2+} complexes were measured using thin glassy films cast from methylene chloride on KBr crystals. Spectra of undiluted $\{Ru(CO)_3Cl_2\}_2$ and the precipitate that

Table 1
Visual observations during the preparation of polymeric ruthenium complexes

Ruthenium (mol%)	Nitrogen purge?	Characteristics of dilute solutions	Characteristics of dried residues
1	Yes	Clear, yellow	Clear, yellow film
1	No	Clear, yellow	Clear, yellow film
2	No	Clear, yellow	Clear, yellow film
3	No	Clear, yellow	Clear, yellow film
5	No	Slightly cloudy, yellow	Cloudy, dark yellow film
10	Yes	Cloudy, yellow	Cloudy, dark yellow film
15	No	Cloudy, yellow	Cloudy, yellow flakes
19	Yes	Cloudy, yellow	Opaque, yellow flakes
20	No	Cloudy, yellow	Opaque, yellow flakes
25	No	Cloudy, yellow	Opaque, yellow flakes
30	No	Cloudy, yellow	Opaque, yellow flakes
50	Yes	Yellow precipitate	Opaque, yellow flakes

contains 50 mol% Ru^{2+} were obtained from cold-pressed powders in a KBr medium at ambient temperature. A Galaxy™ series model 5020 FT-IR, from Mattson Instruments, was employed to perform the desired task. The optical bench is interfaced to a 486/50 MHz personal computer for data acquisition and control. Each spectrum was generated by signal averaging 64 interferograms at a resolution of 4 cm^{-1} and a triangular apodization smoothing function was employed prior to Fourier transformation. A heated transmission cell for solid films from Spectra-Tech (model HT-32) was employed to obtain spectra above ambient. Temperature control was accomplished using a Eurotherm 818P15 programmable microprocessor with an accuracy of ±1°C.

3. Results and discussion

3.1. Effect of transition-metal coordination on the glass transition temperature of poly(4-vinylpyridine)

Dichlorotricarbonylruthenium(II) thermally decomposes at 208°C [24]. Consequently, DSC results above this temperature could not be interpreted very reliably. At a heating rate of 20°C min^{-1}, the undiluted dimer exhibits an exotherm with an onset at 217°C and a peak at 229°C, as illustrated in Fig. 3(a). This exotherm is attributed to thermal decomposition, as described above. When P4VP/Ru^{2+} complexes contain less than 5 mol% Ru^{2+}, two exotherms are observed during the first DSC heating scan (i) between 130°C and 160°C and (ii) at 240–250°C, as illustrated in Fig. 3(b). Since the exotherm between 130°C and 160°C is observed in undiluted poly(4-vinylpyridine) during the first heating, as illustrated in Fig. 3(c), it is not due to the presence of the ruthenium salt. When complexes are heated above 250°C during the first heating trace, (i) no glass transition temperature is evident during the second and subsequent heating scans and (ii) volatilization occurs, as evidenced by deposits of condensed residue in the calorimeter. When complexes are heated above the first exotherm (130–160°C) to 200°C, but below the second exotherm at ≈ 245°C, it is possible to measure the glass transition temperature during subsequent heating traces. The data in Fig. 4 illustrate the synergistic effect of very low Ru^{2+} concentrations on the T_g of poly(4-vinylpyridine). The enhancement in T_g (i.e., ΔT_g), with respect to 145°C for the undiluted polymer, is 9°C at 1 mol% Ru^{2+}, 20°C at 2 mol% Ru^{2+} and 27°C at 3 mol% Ru^{2+}. These enhancements in T_g are significant, particularly when one considers the low concentrations of $\{RuCl_2(CO)_3\}_2$ employed herein, in comparison with previous studies of the same polymer using nickel acetate tetrahydrate [12], cobalt chloride hexahydrate [4] and zinc acetate dihydrate [20]. All of the current and previous T_g data for transition metal coordination complexes with poly(4-vinylpyridine) are summarized in Fig. 4. Based on DSC data for these four systems, divalent ruthenium produces the largest enhancement in T_g per mol% salt.

After each DSC experiment, the sample pan was opened at ambient temperature to observe whether (i) colour changes occurred and whether (ii) the sample was actually heated above its glass transition temperature, as evidenced by fusing and/or flow. All P4VP/Ru^{2+} complexes retain a yellowish colour after they are subjected to 200°C for a few minutes. It was also evident that the particles and/or flakes from the 1–3 mol% Ru^{2+} samples fused together during the DSC experiments, indicating that the glass transition temperature was surpassed. When the concentration of Ru^{2+} exceeds 5 mol%, no T_g is observed below 200°C during the second heating trace, after samples are exposed to 200°C during the first heating scan. The particles and/or flakes in these samples did not fuse together during the DSC experiment, indicating that T_g is above 200°C. Furthermore, when samples containing at least 5 mol% Ru^{2+} are exposed to 300°C during the first heating trace, no glass transition is observed below 270°C during the second heating scan. To support these measurements, visual observations reveal that samples containing at least 5 mol% Ru^{2+} are somewhat darker than the original yellowish complexes and they do not fuse together or flow after being subjected to temperatures near 300°C. Hence, one concludes that P4VP/Ru^{2+} complexes with at least 5 mol% Ru^{2+} do not exhibit a glass transition before the onset of thermal decomposition.

4. Detection of complex formation via infrared spectroscopy

4.1. Pyridine CN stretches

Previous infrared studies of transition metal coordination with monomeric [9] and polymeric [20, 25] pyridine ligands have identified characteristic blue shifts for the in-plane CN stretching vibration of the pyridine ring by 15 or 20 wavenumbers relative to the ''free'' CN stretch at 1598 cm^{-1}. The data in Fig. 5 are consistent with these earlier studies. Infrared spectra of undiluted poly(4-vinylpyridine), the undiluted ruthenium dimer and various P4VP/Ru^{2+} complexes focus on the CN stretch in the pyridine ring near 1600 cm^{-1}. The concentration of Ru^{2+} in these complexes varies from 0.5 mol% to 50 mol%. At 10 mol% Ru^{2+}, a signal is detected at 1637 cm^{-1} which increases in intensity at higher Ru^{2+} concentrations. This signal is characteristic of the undiluted ruthenium dimer which exhibits a broad absorption band in the vicinity of 1630 cm^{-1}, as illustrated in the upper spectrum of Fig. 5. When the Ru^{2+} concentration is at least 5 mol%, an infrared absorption is detected at 1615 cm^{-1} due to in-plane CN stretching of pyridine rings which are coordinated to ruthenium. The intensity of this signal increases at higher Ru^{2+} concentrations. The inset in Fig. 5 illustrates the effect of subtracting the spectrum of undiluted P4VP from spectra of the complexes that contain 1 mol% and 2 mol% Ru^{2+}. These spectral subtractions in the inset clearly identify a signal at 1615 cm^{-1}, even though

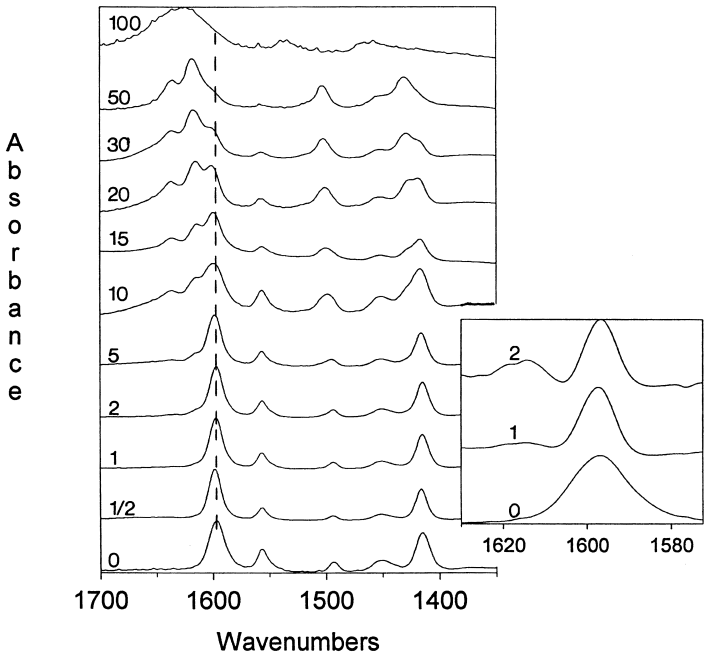

Fig. 5. Infrared spectra between 1350 cm^{-1} and 1700 cm^{-1} for undiluted poly(4-vinylpyridine) (lowest spectrum), the undiluted ruthenium dimer (uppermost spectrum), and several P4VP/Ru^{2+} complexes focusing on carbon–nitrogen and carbon–carbon in-plane stretching vibrations of a pyridine ring which is substituted in the 4-position by the vinyl backbone of the polymer. The mol% of Ru^{2+} is indicated at the left of each spectrum. The dashed line at 1598 cm^{-1} identifies the CN absorption of ''free'' pyridines. This signal shifts 15–20 cm^{-1} to higher energy in the polymeric ruthenium complexes. Spectral subtractions in the inset identify coordinated CN stretches for complexes that contain 1 mol% and 2 mol% Ru^{2+}. These ''difference'' spectra in the inset were obtained by subtracting the spectrum of undiluted P4VP from those of the complexes.

it is difficult to detect this weak signal in the unsubtracted spectra at 1 mol% and 2 mol% Ru^{2+}. Hence, there are also characteristic blue shifts for the in-plane CN stretch of coordinated pyridine rings in the polymer at very low concentrations of Ru^{2+}. The appearance of an infrared absorption at 1615 cm^{-1} has been observed in poly(4-vinylpyridine) coordination complexes with (i) cobalt chloride hexahydrate [26], (ii) zinc acetate dihydrate [20,27], (iii) zinc laurate [20] and (iv) a zinc-neutralized copolymer of ethylene and methacrylic acid [25,27], which is produced commercially by DuPont. Belfiore et al. [20,25] and Gill et al. [28] have suggested that the CN bond is strengthened by π-back-donation of electron density from ruthenium to the π-bonding molecular orbitals of the pyridine ring. If there is sufficient t_{2g}-π orbital overlap, then the pyridine CN bond could be strengthened, producing blue shifts which are observed in the infrared spectra of Fig. 5.

4.2. Model predictions of ''free'' versus complexed pyridines

At 20 mol% Ru^{2+}, the infrared signals at 1615 cm^{-1} and 1598 cm^{-1} exhibit approximately the same absorbance (see Fig. 5). At 30 mol% and 50 mol% Ru^{2+}, the absorbance at 1615 cm^{-1} is stronger than the original uncomplexed signal at 1598 cm^{-1}. If (i) all ruthenium dimers are cleaved at the dichloride bridge and (ii) all metal centers coordinate to two pyridine sidegroups in the polymer, then 20 mol% Ru^{2+} represents the mixture composition at which equal numbers of coordinated and ''free'' pyridine sidegroups coexist. The absorption intensities at 1615 cm^{-1} and 1598 cm^{-1} suggest that there are approximately equal populations of complexed and uncomplexed pyridine sidegroups at 20 mol% Ru^{2+}, if the molar absorption coefficients are the same for both types of pyridines. At higher Ru^{2+} concentrations, one expects that the fraction of complexed pyridines should increase at the expense of ''free'' pyridines. Fig. 6 illustrates model predictions and experimental data from infrared spectroscopy for net absorbance peak heights at 1615 cm^{-1} (complexed pyridines) and 1598 cm^{-1} (uncomplexed pyridines) versus the molar concentration of Ru^{2+}. Each solid line in Fig. 6 corresponds to a different integer number (from one to six) of pyridines in the first-shell coordination sphere of the transition metal. The solid line furthest to the right represents one pyridine per ruthenium and the solid line furthest to the left represents six pyridines per ruthenium. For example, at 10 mol% Ru^{2+}, the pyridine/Ru^{2+} molar ratio is 9:1. If each ruthenium center coordinates to one pyridine sidegroup, then the molar ratio of complexed to free pyridines is 1:8 or 0.125. If two pyridines coordinate to each ruthenium center at 10 mol% Ru^{2+}, then the molar ratio of complexed to free pyridines is 2:7 or 0.285. In general, the molar ratio of complexed to free pyridines is given by $\xi\beta/\{1-(1+\beta)\xi\}$, where ξ is the mole fraction of Ru^{2+} and β is the number of pyridines in the first-shell coordination sphere of the transition metal. These calculations were performed over the following range of Ru^{2+} mole fractions; $0 \leq \xi < (1+\beta)^{-1}$, where the only species

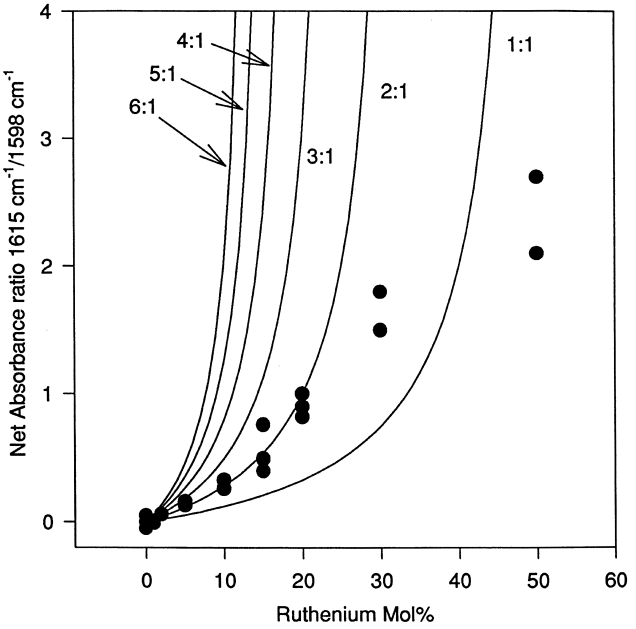

Fig. 6. Molar ratio of coordinated to free pyridines versus mol% of Ru^{2+} in complexes with poly(4-vinylpyridine). Experimental data (circles) were obtained from the infrared spectra in Fig. 5 by taking the ratio of peak absorbances at 1615 cm^{-1} and 1598 cm^{-1}. Model predictions (solid lines) are based on an integer number of pyridines in the first-shell coordination sphere of ruthenium, given by the number associated with each curve, after the dichloride bridge is cleaved.

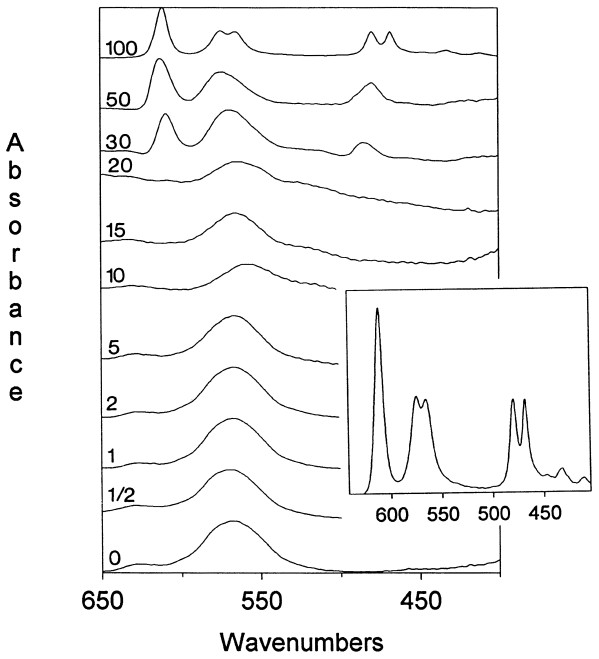

Fig. 7. Infrared spectra between 400 cm^{-1} and 650 cm^{-1} for undiluted poly(4-vinylpyridine) (lowest spectrum), the ruthenium dimer (uppermost spectrum), and several P4VP/Ru^{2+} complexes, focusing on ruthenium–carbon stretches and R–C≡O deformations. The mol% of Ru^{2+} is indicated at the left of each spectrum. The spectrum of the undiluted ruthenium dimer in the low-frequency region is also presented in the inset.

present are (i) Ru^{2+} complexes with the appropriate number of pyridine sidegroup ligands, and (ii) ''free'' pyridines. Fig. 6 illustrates that the infrared data match the model predictions corresponding to $\beta = 2$ when the Ru^{2+} concentration is 20 mol% or less. At 30 mol% Ru^{2+}, the data lie between the predictions for $\beta = 2$ and $\beta = 1$. At 50 mol% Ru^{2+}, the infrared data lie to the right of the predictions for $\beta = 1$, which suggests that the average value of β is less than one, due to the presence of ''free'' ruthenium dimer. Hence, experimental data and model predictions suggest that more than one phase exists at high Ru^{2+} concentrations. Additional evidence, based on metal–carbonyl bands at low frequency, is presented below to support this claim.

4.3. Other pyridine sidegroup absorptions

There are three other characteristic infrared bands for poly(4-vinylpyridine) shown in Fig. 5, at 1415, 1494 and 1558 cm^{-1}, which experience blue shifts or disappear completely at higher Ru^{2+} concentrations. The reason for these blue shifts and signal annihilations in the pyridine region of the infrared spectrum is a consequence of metal-ligand coordination [4,20,25–30]. However, a detailed molecular explanation is not available.

4.4. Metal–carbonyl infrared bands at low frequency

Chemical applications of group theory for a molecule with C_{2h} symmetry (see Fig. 1(A)) suggest that nine infrared-active absorptions are possible for the ruthenium dimer in the low-frequency region of the spectrum [9]. Eight signals are observed in the upper spectrum in Fig. 7 at 610, 576, 565, 476, 464, 448, 436 and 411 wavenumbers, corresponding to Ru–C≡O deformations and ruthenium–carbon stretches. The higher frequency bands are attributed to Ru—C≡O deformations and the lower frequency signals correspond to ruthenium–carbon stretches [9]. The spectra in Fig. 7 present low-frequency infrared absorptions for the undiluted polymer, the undiluted ruthenium dimer and various P4VP/Ru^{2+} complexes. The absorption at 610 cm^{-1} and all five signals below 500 cm^{-1} are absent in polymeric complexes that contain 20 mol% Ru^{2+} or less. The two signals at 576 cm^{-1} and 565 cm^{-1} are partially resolved in the ruthenium dimer, but this resolution is obscured by a broad absorption of poly(4-vinylpyridine) at 570 cm^{-1} in all of the complexes. At 30 and 50 mol% Ru^{2+}, the signal at 610 cm^{-1} is characteristic of the undiluted dimer. This observation supports the conclusion based on infrared data in the pyridine CN stretching region. Hence, there is infrared evidence near 600 cm^{-1} and 1600 cm^{-1} that more than one phase coexists at high Ru^{2+} concentrations.

4.5. Carbonyl absorptions of the ruthenium salt

Fig. 8 illustrates the infrared spectral region between 1850 cm^{-1} and 2200 cm^{-1} for the undiluted ruthenium

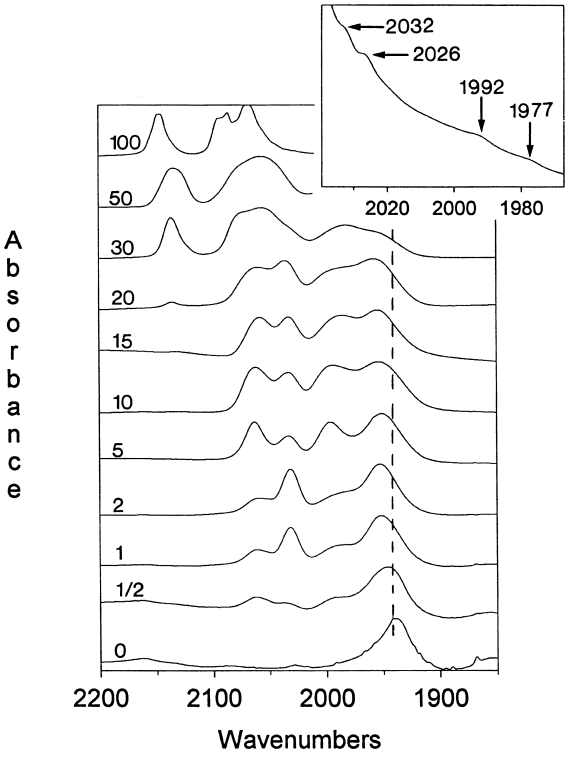

Fig. 8. Infrared spectra between 1800 cm^{-1} and 2200 cm^{-1} for undiluted poly(4-vinylpyridine) (lowest spectrum), the undiluted ruthenium dimer (uppermost spectrum) and several P4VP/Ru^{2+} complexes. The mol% of Ru^{2+} is indicated at the left of each spectrum. Weak C≡O absorptions of the undiluted dimer are identified in the inset. Multiple C≡O stretching modes and the effect of π-backbonding are used to postulate the structure of the complexes. The dashed line at 1940 cm^{-1} corresponds to a signal for undiluted P4VP that was not included in the symmetry analysis of the CO stretches.

dimer, undiluted poly(4-vinylpyridine), and various P4VP/Ru^{2+} complexes. Except for the polymer signal at 1940 cm^{-1}, identified by the dashed line, the remaining signals correspond to carbonyl stretches in the ruthenium salt. There are no CO absorptions between 1750 cm^{-1} and 1900 cm^{-1} that indicate bridging to two ruthenium centers [10]. The infrared data in Fig. 8 are useful for identifying the number of terminal CO ligands and the geometry of the complexes via symmetry considerations. The strongest carbonyl absorptions of dichlorotricarbonylruthenium(II) dispersed in KBr occur at 2147, 2095, 2086 and 2069 cm^{-1}. There are also some weaker signals at 2032, 2026, 1992 and 1977 cm^{-1}, as illustrated in the inset to Fig. 8. Eight infrared-active CO stretches are consistent with the simultaneous existence of two isomers of the ruthenium dimer [31]. When all chloride and carbonyl ligands adopt a *cis*-arrangement, the dimer exhibits C_{2h} symmetry with a center of inversion, as illustrated in Fig. 1(A). In this case, there are three infrared-active C≡O stretches that belong to the following irreducible representations in C_{2h}; $A_u + 2B_u$. The other isomer contains some chlorides and some carbonyls in a *trans*-arrangement (i.e., C_{2v} symmetry), as shown in Fig. 1(B). Now, there are five infrared-active C≡O stretches that transform as $2A_1 + 2B_1 + B_2$ in the C_{2v} point group. Benedetti et al. [9] report that the carbonyl absorptions of $\{RuCl_2(CO)_3\}_2$ occur at 2140, 2092 and 2066 cm^{-1} for the isomer with C_{2h} symmetry. Similarly, Cleare and Griffith [32] report that these absorptions of the dimer with C_{2h} symmetry occur at 2148, 2088 and 2068 cm^{-1} in the solid state.

5. Analysis of infrared spectroscopic data of the carbonyl ligands via molecular symmetry

5.1. Proposed structures for P4VP–ruthenium complexes

Symmetry analysis reveals that a mono-nuclear complex with a single metal center exhibits a unique stretching vibration for each CO ligand if the molecular point group does not contain either (i) the center of inversion or (ii) a three-fold or higher proper rotation axis [10,33]. In other words, molecules that are highly symmetric will have fewer CO infrared absorptions than the number of CO ligands [10]. Benedetti et al. [9] report that CO absorptions occur at 2070 and 2006 cm^{-1} for a methylene chloride solution of $RuCl_2(CO)_2(C_5H_5N)_2$, where both chloride ligands are *trans*-, and the carbonyl and pyridine ligands are in a *cis*-arrangement. This is the first entry (i.e., (b)) with C_{2v} symmetry in Table 2. The 2140 cm^{-1} signal is absent in $RuCl_2(CO)_2(C_5H_5N)_2$. If two isomers of the ruthenium dimer exist simultaneously, as discussed above and illustrated in Fig. 1, then five different ligand arrangements about a single ruthenium center are

Table 2
Geometrical arrangements and symmetry considerations for $RuCl_2(CO)_2(Py)_2$

Isomer	Point group	Cl^- ligands	Py[a] ligands	CO ligands	Number of infrared-active CO stretches and symmetry types
(a)	C_1	*cis*-	*cis*-	*cis*-	2 [A + A]
(b)	C_{2v}	*trans*-	*cis*-	*cis*-	2 [$A_1 + B_1$]
(c)	C_{2v}	*cis*-	*trans*-	*cis*-	2 [$A_1 + B_1$]
(d)	C_{2v}	*cis*-	*cis*-	*trans*-	1[b] [$A_1 + B_1$]
(e)	D_{2h}	*trans*-	*trans*-	*trans*-	1 [B_{2u}]

[a] Py is an acronym for the pyridine sidegroup in poly(4-vinylpyridine).
[b] See explanation in the text for the reason why 2 C≡O stretches are not observed [10].

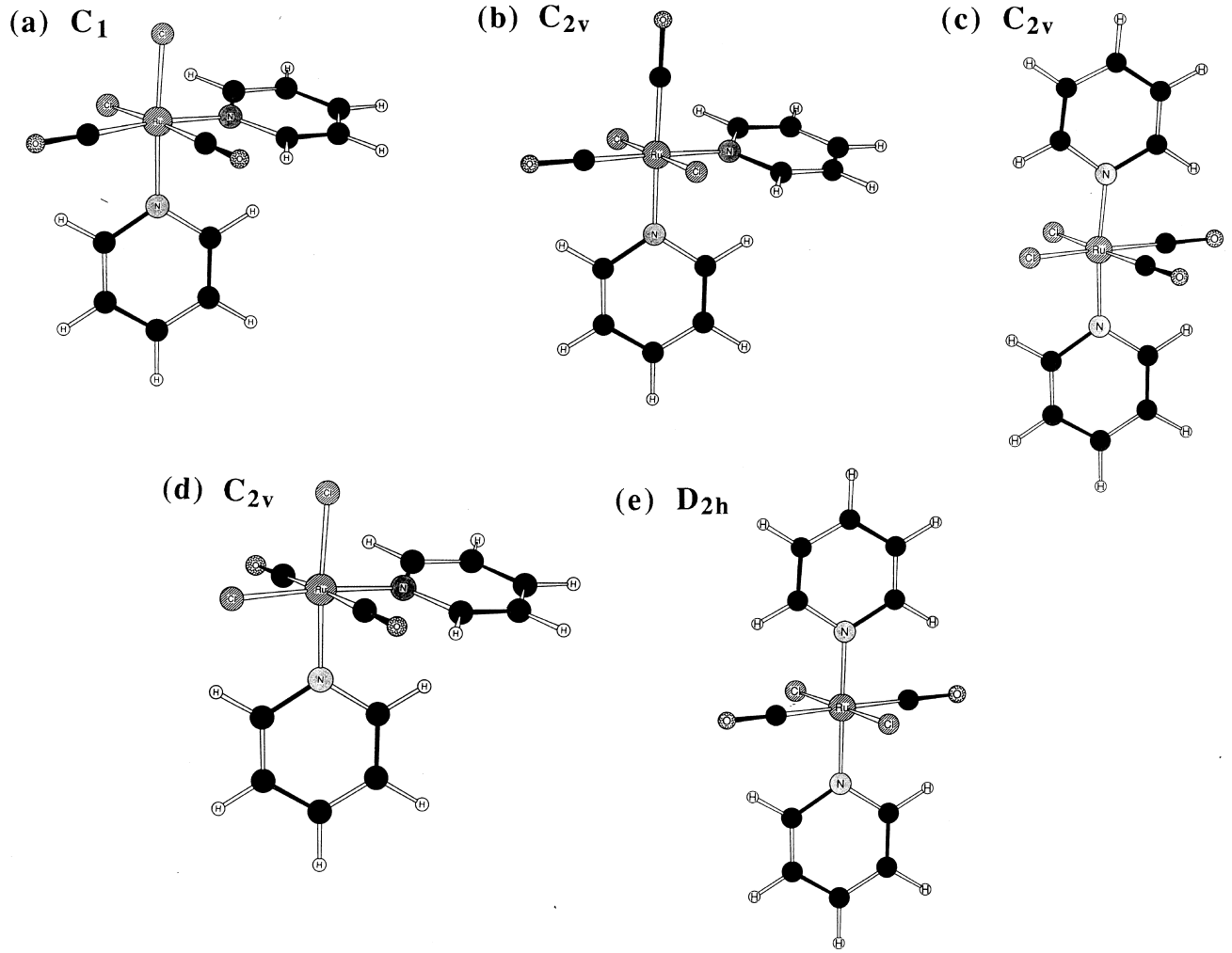

Fig. 9. Five isomers of $RuCl_2(CO)_2(C_5H_5N)_2$ with a single ruthenium center. Pyridine sidegroups in P4VP (i) cleave the dichloride bridge, (ii) occupy the vacant site in the coordination sphere of the metal and (iii) displace one CO ligand. Local point group symmetry is included. The expected number of C≡O stretches and the irreducible representations to which they belong are provided in Table 2 for each isomer.

possible for $RuCl_2(CO)_2(Py)_2$ after the dimer is cleaved by the polymeric sidegroups. These five ligand arrangements are illustrated in Fig. 9 and Table 2, together with their corresponding point groups. ''Py'' is used as an acronym for pyridine sidegroups coordinated to ruthenium via the nitrogen lone pair. Four ligand arrangements in Fig. 9(a–d), which correspond to the first four entries in Table 2, do not possess a center of inversion. For the first three entries in Table 2, the carbonyl ligands are in a *cis*-configuration and two CO signals should appear in the infrared spectrum for each of these complexes. When both CO ligands are in a *trans*-arrangement, as illustrated by configuration (d) in Fig. 9, with C_{2v} symmetry, it is possible that colinearity of the CO ligands will generate one CO infrared signal [10], even though a center of inversion or proper rotation axis $\leq 120^\circ$ does not exist. When all identical ligands are *trans*-, the molecule exhibits D_{2h} symmetry, as shown in Fig. 9(e), and possesses a center of inversion. Hence, only one carbonyl absorption (i.e., B_{2u}) should appear in the infrared spectrum of this complex, identified by the last entry in Table 2. Infrared spectra of the P4VP/Ru^{2+} complexes in Fig. 8 exhibit three carbonyl signals (2057–2063 cm^{-1}, 2032 cm^{-1} and 1985–1990 cm^{-1}) at concentrations below 20 mol% Ru^{2+}, and four signals (2136 cm^{-1}, 2057–2063 cm^{-1}, 2032 cm^{-1} and 1985–1990 cm^{-1}) when the Ru^{2+} concentration is 20 mol% or higher. The two absorptions at ≈1987 and 2060 cm^{-1} are not very different from those at 2006 and 2070 cm^{-1} in a methylene chloride solution of $RuCl_2(CO)_2(C_5H_5N)_2$, as reported by Benedetti et al. [9]. These signals at 1987 cm^{-1} and 2060 cm^{-1} are assigned to the two carbonyl absorptions for P4VP/Ru^{2+} complexes that have ligand arrangements described by the first three entries in Table 2, in which the CO ligands are in a *cis*-configuration. This is consistent with the assignments given by Benedetti et al. [9] and Bruce and Stone [31]. The CO absorption at 2032 cm^{-1} is assigned to $RuCl_2(CO)_2(C_5H_5N)_2$ with either C_{2v} or D_{2h} symmetry when both CO ligands are *trans*- to each other. Based on

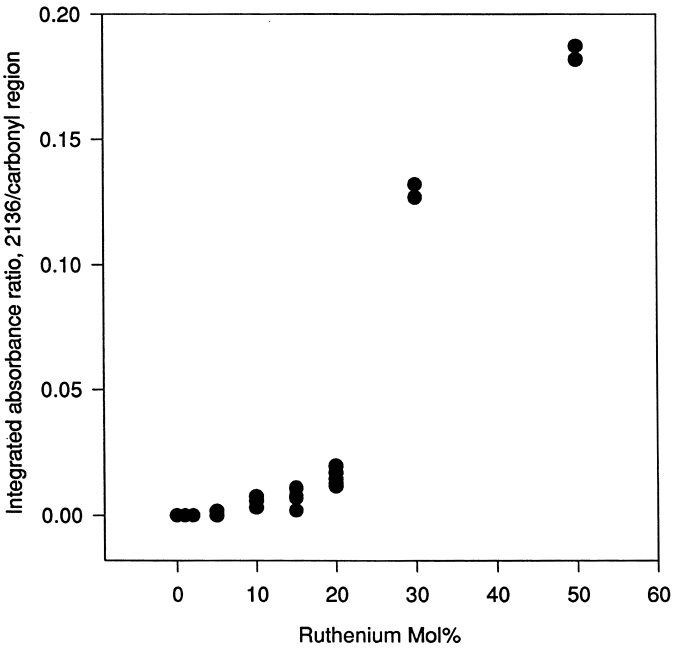

Fig. 10. Mole fraction of $RuCl_2(CO)_3(C_5H_5N)$ via the CO stretch at 2136 cm^{-1} versus the total mol% of Ru^{2+} in coordination complexes with poly(4-vinylpyridine). Experimental data were obtained from the infrared spectra in Fig. 8 by taking the ratio of the integrated absorbance at 2136 cm^{-1} with respect to the integrated absorbance of the entire carbonyl region.

these assignments, simultaneous existence of at least two $RuCl_2(CO)_2(C_5H_5N)_2$ isomers with either (i) C_1 and C_{2v}, (ii) C_1 and D_{2h}, (iii) C_{2v} and C_{2v} or (iv) C_{2v} and D_{2h} symmetries represents the most plausible explanation for three carbonyl signals in Fig. 8 when the concentration of Ru^{2+} is less than 20 mol%. This explanation is consistent with the spectrum of the pure dimer at the top of Fig. 8 which shows evidence for the simultaneous existence of two isomers, as illustrated in Fig. 1. Three carbonyl signals are also possible if $RuCl_2(CO)_3(C_5H_5N)$ is present. This complex might exist if the polymer cleaves the dichloride bridge and one pyridine sidegroup occupies the vacant site in the coordination sphere of ruthenium without displacing any CO ligands. Benedetti et al. [9] have recorded the carbonyl absorptions of $RuCl_2(CO)_3(C_5H_5N)$ at 2136, 2075 and 2051 cm^{-1}. As expected, the CO absorptions at 2075 and 2051 cm^{-1} in $RuCl_2(CO)_3(C_5H_5N)$ occur at higher energy, relative to the CO absorptions in *cis*-$RuCl_2$-$(CO)_2(C_5H_5N)_2$, because there is a smaller amount of π-back-donation into the π*-antibonding orbitals of CO from only one pyridine σ-donor ligand. Infrared signals at 2136, 2075 and 2051 cm^{-1} are absent when the Ru^{2+} concentration is less than 20 mol% in Fig. 8, suggesting that $RuCl_2(CO)_3(C_5H_5N)$ does not exist in this concentration regime. This conclusion is consistent with the organometallic literature of small-molecules [9] because an excess of pyridine cleaves the dichloride bridge of the ruthenium dimer, one pyridine occupies the vacant site after cleavage and another pyridine displaces carbon monoxide.

The carbonyl absorption at 2136 cm^{-1} appears initially in Fig. 8 when the concentration of Ru^{2+} is 20 mol% and the intensity of this signal increases at 30 mol% and 50 mol% Ru^{2+}. Following Benedetti et al. [9], the CO stretch at 2136 cm^{-1} is consistent with the existence of $RuCl_2(CO)_3(C_5H_5N)$, even though poor spectral resolution hinders the detection of CO stretches at 2075 and 2051 cm^{-1} which are also characteristic of this complex with one pyridine ligand. Fig. 10 shows the net integrated absorbance of the 2136 cm^{-1} signal relative to the total integrated absorbance of all CO stretches as a function of the molar concentration of Ru^{2+}. Measurable amounts of the 2136 cm^{-1} signal appear at 20 mol% Ru^{2+}, and this signal becomes quite significant at 30 mol% and 50 mol% Ru^{2+}. This corresponds well with the data in Fig. 6 which illustrate that there are less than two pyridines coordinated to the metal center at 30 mol% and 50 mol% Ru^{2+}. Thus, both the carbonyl and pyridine CN stretching regions of the infrared spectrum suggest that there is a significant fraction of $RuCl_2(CO)_3(C_5H_5N)$ when the concentration of Ru^{2+} is greater than 20 mol%.

5.2. High-temperature infrared spectroscopy of polymeric ruthenium complexes

It is not uncommon for ligand rearrangements to occur at elevated temperatures [34]. In some cases, molecular symmetry can be invoked to explain these rearrangements by monitoring the carbonyl absorptions as a function of temperature. The data in Fig. 11 illustrate infrared spectra at 7 different temperatures between 30°C and 200°C for the P4VP/Ru^{2+} complex which contains 2 mol% Ru^{2+}. Similar data are presented in Fig. 12 at 5 different temperatures between 30°C and 180°C when the Ru^{2+} concentration is 20 mol%. The data in Figs 6 and 10 indicate that the fraction

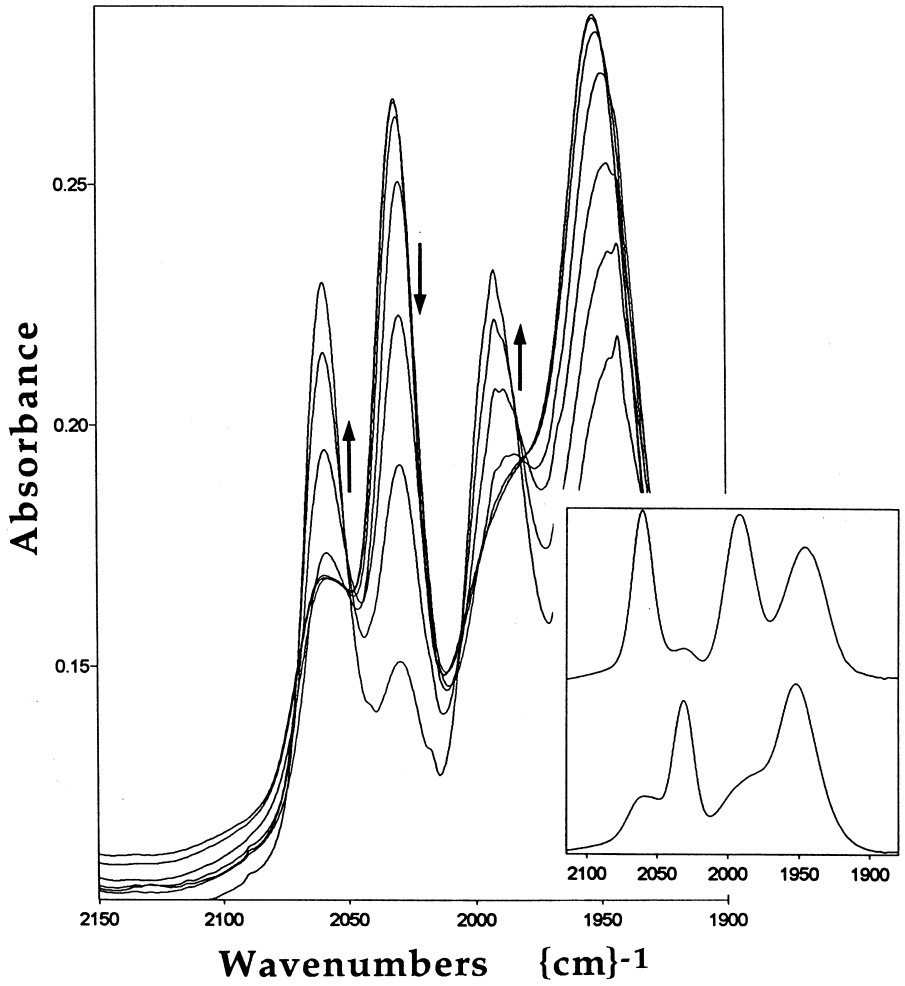

Fig. 11. High-temperature infrared spectra between 30°C and 200°C in the CO stretching region for a P4VP/Ru^{2+} complex that contains 2 mol% Ru^{2+}. Arrows indicate the effect of increasing temperature. The actual temperatures are 30°C, 50°C, 100°C, 150°C, 165°C, 180°C and 200°C. The inset presents ambient-temperature infrared spectra in the CO stretching region for the same P4VP/Ru^{2+} complex before (lower) and after (upper) heat treatment at 200°C.

of $RuCl_2(CO)_3(C_5H_5N)$ is insignificant until the Ru^{2+} concentration reaches 30 mol%. Hence, it is reasonable to assume that $RuCl_2(CO)_2(C_5H_5N)_2$ is the primary complex at 20 mol% Ru^{2+} because the experimental data in Fig. 6 agree with simulations when two pyridines occupy sites in the coordination sphere of ruthenium (i.e., $\beta = 2$). Based on symmetry analysis of the infrared spectra in Fig. 8, at least two different $RuCl_2(CO)_2(C_5H_5N)_2$ isomers, and as many as five, exist simultaneously. Isomers with C_1 and C_{2v} symmetry and no center of inversion (i.e., the first three entries in Table 2) exhibit two carbonyl absorptions at 1987 cm^{-1} and 2060 cm^{-1}. Isomers with C_{2v} and D_{2h} symmetry which have both CO ligands in a *trans*-arrangement (i.e., the last two entries in Table 2) exhibit only one carbonyl absorption at 2032 cm^{-1}. The arrows in Figs 11 and 12 indicate that (i) the signal at 2032 cm^{-1} *decreases* significantly at higher temperature when the Ru^{2+} concentration is 2 mol% and 20 mol%, and (ii) the signals at 1987 cm^{-1} and 2060 cm^{-1} *increase* significantly at higher temperature when the Ru^{2+} concentration is 2 mol%, but not 20 mol%. The effect of temperature on these infrared signal intensities is irreversible, as illustrated in the insets of Figs 11 and 12, because the upper spectrum in each inset was acquired at ambient temperature after both samples were exposed to 200°C for 15 minutes. Obviously, the 2032 cm^{-1} absorption for $RuCl_2(CO)_2(C_5H_5N)_2$ isomers with *trans*-CO ligands decreases after high-temperature heat treatment, whereas the C≡O signals for the complexes of lower symmetry increase. This suggests very strongly that irreversible ligand rearrangements to lower symmetry occur when $RuCl_2(CO)_2(C_5H_5N)_2$ is heated to 200°C. To verify that the redistribution of CO absorption intensities shown in Figs 11 and 12 is due to temperature-induced ligand rearrangements rather than the loss of CO via dissociation (i.e., thermal ejection) or thermal degradation, the net integrated absorbance of the carbonyl region relative to the total integrated absorbance of the entire spectrum (i.e., 400–4000 cm^{-1}) is presented in Fig. 13 as a function of Ru^{2+} concentration. The triangular data points with error bars summarize spectral information obtained from samples that were not

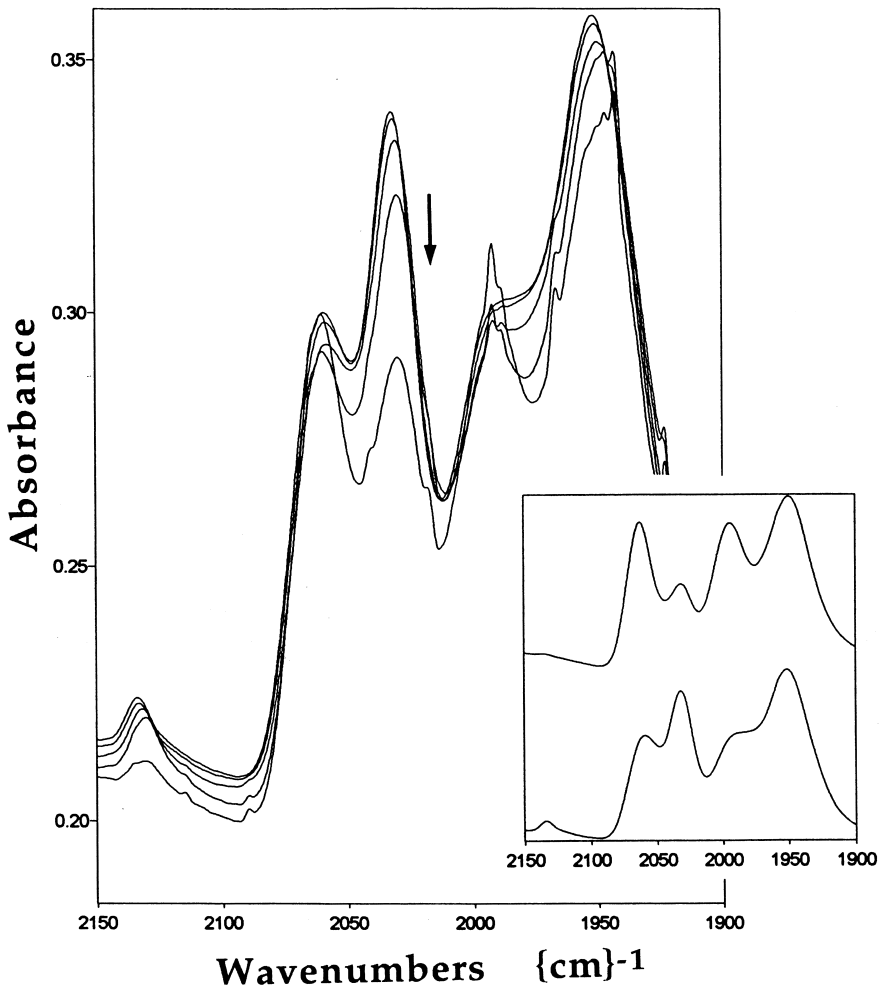

Fig. 12. High-temperature infrared spectra between 30°C and 180°C in the CO stretching region for a P4VP/Ru^{2+} complex which contains 20 mol% Ru^{2+}. The effect of increasing temperature on the signal intensity at 2032 cm^{-1} is indicated by the arrow. The actual temperatures are 30°C, 50°C, 100°C, 150°C and 180°C. The inset presents ambient-temperature infrared spectra in the CO stretching region for the same P4VP/Ru^{2+} complex before (lower) and after (upper) heat treatment at 200°C.

exposed to elevated temperatures. The linear least-squares regression line is $y = 0.88x + 0.038$, where y is the net integrated absorbance of the CO stretching region relative to the total integrated absorbance of the entire spectrum, and x is the mole fraction of Ru^{2+} in complexes with poly(4-vinylpyridine). The integrated absorbances of the low frequency vibrations between 410 cm^{-1} and 610 cm^{-1} due to Ru–C≡O deformation and Ru–C stretching do not contribute significantly to the mole fraction of CO ligands. The correlation in Fig. 13 directly monitors the concentration of Ru^{2+} in these polymeric complexes. After subjecting P4VP/Ru^{2+} complexes to 200°C for 15 min, the circular data points indicate that the relative integrated absorbances of the CO stretches at ambient temperature are very close to the original data for complexes that have not been exposed to high temperature. The data in Fig. 13 provide justification for the claim that heat treatment at 200°C does not eject CO or degrade P4VP/Ru^{2+} complexes. Hence, irreversible ligand rearrangements which occur at elevated temperature (i.e., 200°C) generate $RuCl_2(CO)_2(C_5H_5N)_2$ complexes with (i) lower symmetry and (ii) fewer CO ligands in a *trans*-configuration. This interpretation is consistent with the high-temperature infrared data in Figs 11 and 12.

6. Conclusions

Transition metal coordination complexes between poly(4-vinylpyridine) and dichlorotricarbonylruthenium(II) exhibit a 27°C enhancement in T_g when the concentration of Ru^{2+} is only 3 mol%. The glass transition cannot be detected above 3 mol% Ru^{2+}, due to complications from thermal degradation. Infrared data from the pyridine side-group in the polymer suggest that the nitrogen lone pair coordinates to the metal center. Symmetry considerations and infrared data for the carbonyl stretching vibrations are consistent with a structural model that places two CO

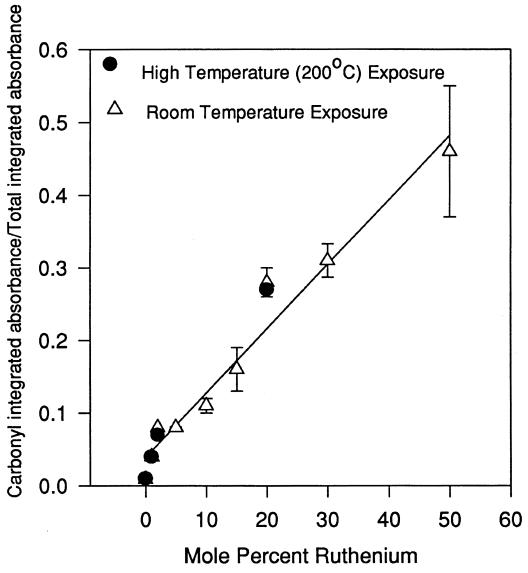

Fig. 13. Mole fraction of CO via integrated absorbance of the entire carbonyl region of the spectrum versus the total mol% of Ru^{2+} in coordination complexes with poly(4-vinylpyridine). All infrared spectra were obtained at ambient temperature. Heat treatment at 200°C for 15 min does not eject CO or degrade the complexes in comparison with similar data (open triangles) for samples that have not been subjected to high temperatures.

ligands and two pyridine sidegroups in the first-shell coordination sphere of ruthenium, as illustrated in Figs 2 and 9, when the concentration of Ru^{2+} is less than 20 mol%. If the transition-metal salt bridges two different chains via the pyridine nitrogen lone pair, forming coordination crosslinks, then this type of hindered mobility provides a reasonable explanation for the enhancement in T_g. There are a few isomers of $RuCl_2(CO)_2(C_5H_5N)_2$ which exist simultaneously and which could represent coordination crosslinks. At elevated temperatures up to 200°C, the highly symmetric isomers with *trans*-CO ligands transform irreversibly to pseudo-octahedral structures of lower symmetry where the CO ligands are *cis*- to each other. When the concentration of Ru^{2+} is greater than 20 mol%, carbonyl and pyridine CN infrared stretches suggest that a significant fraction of $RuCl_2(CO)_3(C_5H_5N)$ exists. On the basis of pyridine CN stretches near 1600 cm^{-1}, model simulations suggest that ''free'' ruthenium dimer is also present at high concentrations of Ru^{2+}. Hence, a multiphase mixture of Ru^{2+} coordination crosslinks $RuCl_2(CO)_2(C_5H_5N)_2$, ruthenium pendant groups on linear polymer chains $RuCl_2(CO)_3(C_5H_5N)$ and uncleaved dimer $\{RuCl_2(CO)_3\}_2$ exists at high concentrations of Ru^{2+} (i.e., $>$ 30 mol%). Octahedral ruthenium d^6 salts are attractive physical property modifiers when at least two polymeric ligands from different chains coordinate to the metal center.

Acknowledgements

The research discussed herein was supported by the National Science Foundation under Grant No. DMR-9528555.

References

[1] Jiang M, Zhou C, Zhang Z. Polymer Bulletin 1993;30:455.
[2] Belfiore LA, Bossé F, Lee JY. ACS Proceedings; Division of Polymeric Materials, Science and Engineering 1996;75:48.
[3] Indra EM, McCurdie MP, Sun X, Belfiore LA. Transition-metal compatibilization of polymer blends. In: Lohse DJ, Russell TP, Sperling, LH, editors. Interfacial aspects of multicomponent polymer materials. New York: Plenum, 1997:241–264.
[4] Belfiore LA, McCurdie MP, Ueda E. Macromolecules 1993;26: 6908.
[5] Belfiore LA, Bossé F, Das P. Polymer International 1995;36 (2):165.
[6] Belfiore LA, Das P, Bossé F. Journal of Polymer Science, Polymer Physics Edition 1996;34:2675.
[7] Belfiore LA, Indra EM, Das P. Macromolecular Symposia—Polymer–Solvent Complexes 1997;114:35.
[8] Merlino S, Montagnoli G. Atti Soc Tosc Scienze Naturali 1970;76:335.
[9] Benedetti E, Braca G, Sbrana G, Salvetti F, Grassi B. Journal of Organometallic Chemistry 1972;37:361.
[10] Shriver DF, Atkins PW, Langford CH. Inorganic chemistry. New York: WH Freeman, 1990:208–9, 212, 505–510.
[11] Figgis BN. An introduction to ligand fields. New York: Wiley, 1966:189–195.
[12] Belfiore LA, Graham HRJ, Ueda E. Macromolecules 1992;25:2935.
[13] Cotton FA, Wilkinson G. Advanced inorganic chemistry—a comprehensive text, 3rd ed. New York: Wiley-Interscience, 1972:100–117.
[14] Pearson RG. In: Scott AF, editor. Survey of progress in chemistry, vol. 5. New York: Academic Press, 1969:12.
[15] Fowkes FM, Tischler DO. Journal of Polymer Science, Polymer Chemistry Edition 1984;22:547.
[16] Forster RJ, Vos JG. Macromolecules 1990;23:4372.
[17] Bourdeland JL, Campa C, Font J, de March P. European Polymer Journal 1989;25 (2):197.
[18] Denti G, Campagna S, Sabatino L, Serroni S, Ciano M, Balzani V. Inorganica Chimica Acta 1990;176:175.
[19] Qin C, Pires ATN, Belfiore LA. Polymer Communications 1990;31:177.
[20] Belfiore LA, Pires ATN, Wang Y, Graham HRJ, Ueda E. Macromolecules 1992;25 (5):1411.
[21] Belfiore LA, Lutz TJ, Cheng CM, Bronnimann CE. Journal of Polymer Science, Polymer Physics Edition 1990;28:1261.
[22] Belfiore LA, Ueda E. Polymer 1992;33:3833.
[23] Belfiore LA, Qin C, Ueda E, Pires ATN. Journal of Polymer Science, Polymer Physics Edition 1993;31:409.
[24] Strem Chemicals Inc. Metals, inorganics and organometallics for research. Catalog No. 17, 1997–99:216.
[25] Belfiore LA, Graham HRJ, Ueda E, Wang Y. Polymer International 1992;28 (1):81.
[26] McCurdie MP. MS Thesis at Colorado State University, 1994:32b.
[27] Wang Y. MS Thesis at Colorado State University, 1991:22,71,77.
[28] Gill NS, Nuttall RH, Scaife DE, Sharp DWA. Journal of Inorganic and Nuclear Chemistry 1961;18:79.
[29] Peiffer DG, Duvdevani I, Agarwal PK. Journal of Polymer Science, Polymer Letters Edition 1986;24:581.
[30] Allan JR, Baird ND, Kassyk AL. Journal of Thermal Analysis 1979;16:79.
[31] Bruce MI, Stone FGA. Journal of the Chemical Society 1967;A:1238.
[32] Cleare MJ, Griffith QP. Journal of the Chemical Society 1969;A:372.
[33] Cotton FA. Chemical applications of group theory, 2nd ed., chap. 10. New York: Wiley Interscience, 1971.
[34] Collman JP, Hegedus LS, Norton JR, Finke RG. Principles and applications of organotransition metal chemistry, chap. 4. Mill Valley, CA: University Sciences Books, 1987.